

# IFIH1 promotes apoptosis through the TBK1/IRF3 pathway in triple-negative breast cancer

Chao SHI<sup>1</sup>, Xiaohan WANG<sup>1</sup>, Jingping LI<sup>2</sup>, Shang WU<sup>1</sup>, Zhihui LIU<sup>3</sup>, Xiaofei REN<sup>1</sup>, Xiangmei ZHANG<sup>2,4,\*</sup>, Yunjiang LIU<sup>1,2,\*</sup>

<sup>1</sup>Department of Breast Center, The Fourth Hospital of Hebei Medical University, Shijiazhuang, China; <sup>2</sup>Hebei Provincial Key Laboratory of Tumor Microenvironment and Drug Resistance, Shijiazhuang, China; <sup>3</sup>Department of Burns and Plastic Surgery, Shijiazhuang People's Hospital, Shijiazhuang, China; <sup>4</sup>Hebei Provincial Cancer Institute, Shijiazhuang, China

\*Correspondence: xiangmeizhang@hebm.u.edu.cn; lyj818326@hebm.u.edu.cn

Received June 14, 2024 / Accepted November 26, 2024

Triple-negative breast cancer (TNBC) is a highly aggressive subtype of breast malignancy. Although some patients benefit from immune checkpoint therapy, current treatment methods rely mainly on chemotherapy. It is imperative to develop predictors of efficacy and identify individuals who will be sensitive to particular treatment regimens. This study analyzed peripheral interferons and immune cell subsets in TNBC patients receiving pre-operative neoadjuvant therapy. The effects of interferon-induced helicase 1 (IFIH1) on the biological characteristics of apoptosis and PD-L1 expression of cancer cells and its potential mechanism were investigated using bioinformatics analysis, clinical specimens, and *in vitro* study. We found that serum interferon- $\gamma$  and interferon- $\alpha 2$  levels were significantly higher in TNBC patients with pathologic complete response (pCR). The expression of IFIH1 is markedly upregulated in various tumors, including breast cancer. Immunohistochemical results revealed that IFIH1 was specifically located in the cytoplasm of cancer cells. Gene set enrichment analysis showed that genes co-expressed with IFIH1 were involved in tumor immune-related pathways and apoptosis. Knockdown of IFIH1 in MDA-MB-231 and BT-549 cells resulted in significantly increased cell proliferation and colony formation. Regarding apoptosis-related pathway proteins, there was a significant decrease in levels of phosphorylated TANK-binding kinase 1 (TBK1) and phosphorylated interferon regulatory factor 3 (IRF3). In addition, the expression of PD-L1 was significantly downregulated. Furthermore, we demonstrated the existence of binding sites between IRF3 and PD-L1 promoters. Our data indicate that cancer cell IFIH1 promotes apoptosis and PD-L1 expression, suggesting its potential as a predictive marker of efficacy and therapeutic target in TNBC.

**Key words:** IFIH1; type I interferon; apoptosis; triple-negative breast cancer; PD-L1

Patients with triple-negative breast cancer (TNBC) have relatively unfavorable prognosis and limited treatment options owing to a lack of suitable endocrine and targeted therapies [1, 2]. The emergence of immunotherapy has brought new hope for treatment [3]. However, the relatively low effectiveness and potential for drug resistance have severely limited its clinical applications in TNBC. Current therapeutic strategies for TNBC mainly depend on chemotherapy, and there is thus an urgent need to develop predictive biomarkers and effective therapeutic targets.

Tumor cells share key features such as oxidative stress, genomic instability and mutations, and changes in metabolic rate; these may lead to nuclear or mitochondrial DNA or RNA damage and the consequent release of damaged nucleic acid fragments into the cytoplasm [4]. Recent studies have shown that cancer cells can mimic viral infections, triggering

RNA-sensing pattern recognition receptors and interferon response pathways [5] and thereby activating cytotoxic immune cells (natural killer cells and CD8+T cells) to destroy them through cell lysis and apoptosis [6]. The interferon-induced helicase (IFIH1) gene, located on chromosome 2q24.3, contains domains essential for the immune response against viral double-stranded RNA (dsRNA), activating a signaling cascade that expresses type I interferons and stimulates an antiviral immune response [7, 8]. Recent studies have shown that targeting IFIH1-related signaling pathways may have broad application prospects in tumor immunotherapy and represents a promising approach to treating cancer via regulation of apoptosis and acquired immunity [9].

We previously reported that elevated serum pro-inflammatory cytokines are associated with increased pathological complete response (pCR) in breast cancer (BC) patients



Copyright © 2024 The Authors.

This article is licensed under a Creative Commons Attribution 4.0 International License, which permits use, sharing, adaptation, distribution, and reproduction in any medium or format, as long as you give appropriate credit to the original author(s) and the source and provide a link to the Creative Commons licence. To view a copy of this license, visit <https://creativecommons.org/licenses/by/4.0/>

receiving neoadjuvant therapy [10]. In this study, we observed that patients who achieved pCR demonstrated significantly higher baseline levels of interferon-gamma (IFN- $\gamma$ ) and interferon-alpha2 (IFN- $\alpha$ 2) prior to treatment compared to non-pCR patients. Thus, we evaluated IFIH1 expression and co-expression networks in TNBC. Finally, through a series of *in vitro* experiments, we confirmed the significant association between IFIH1 expression and tumor cell proliferation and apoptosis, elucidating its potential regulatory mechanisms.

## Materials and methods

### Blood cytokines and immune cell subsets evaluation.

The plasma levels of 5 inflammatory cytokines and 4 peripheral blood immune cell subsets in 8 patients with TNBC who underwent preoperative neoadjuvant chemotherapy and surgical resection were evaluated before treatment.

Peripheral blood samples from patients were collected before treatment. Samples were centrifuged (1,000 $\times$ g) for 15 min to separate serum, and the expressions of five cytokines (IL-1 $\beta$ , IFN- $\alpha$ 2, IFN- $\gamma$ , TNF- $\alpha$ , IL-6) were detected by using the Cytometric Bead Array kit (Becton Dickinson, USA). Immune cell subpopulations were directly assessed in peripheral blood samples by using flow cytometry and related antibodies (BD Bioscience).

**Bioinformatics analysis.** TIMER2.0 (<http://timer.cistrome.org>) [11] was used to investigate the different expression profiles of IFIH1 between pan-cancer and adjacent normal tissues. The gene expression levels were shown using a log<sub>2</sub> (TPM+1) scale, where TPM stands for transcripts per million. UALCAN (<http://ualcan.path.uab.edu/index.html>) [12] database was used to analyze the relationship between IFIH1 expression and molecular subtypes of breast cancer. The Human Protein Atlas (HPA) (<http://www.proteinatlas.org/>) [13] was further used to confirm the intensity of IFIH1 immunohistochemical staining in BC tumors and normal tissues.

Kaplan-Meier Plotter (<https://kmplot.com>) [14] was used to evaluate the prognostic significance of IFIH1 expression in TNBC. Similarly, the cohorts were divided into two groups according to the median expression of IFIH1 and were compared in terms of relapse-free survival (RFS) and overall survival (OS). The hazard ratios (HRs) were computed with 95% CIs and log-rank p-values.

Expression profiles (HTSeq-TPM) were compared between the high and low IFIH1 mRNA expression groups in BC from The Cancer Genome Atlas (TCGA) database to identify the differentially expressed genes (DEGs) using the unpaired Student's t-test.  $|\log_2 \text{Fold Change}| > 1.5$  and adjusted  $p < 0.05$  are the DEGs threshold. The STRING database (<https://string-db.org>) was used to construct the protein-protein interaction network of IFIH1 in BC. The potential biological function of IFIH1 expression on the prognosis of BC was investigated by GSEA analysis. After

correction, functional pathways with  $p < 0.05$ , error finding rate (FDR)  $< 0.25$ , and standardized enrichment score (NES)  $> 1$  were considered significantly enriched.

**Tissue samples and immunohistochemistry.** IFIH1 and PD-L1 expression was analyzed immunohistochemically on paraffin-embedded tumor sections (39 BC tissues) using rabbit anti-human IFIH1 polyclonal antibody (Proteintech, 21775-1-AP) and PD-L1 antibody (Proteintech, 28076-1-AP). All patients underwent one-stage operation. This study was approved by the Institutional Ethics Committee of the Fourth Hospital of Hebei Medical University (Approval no: 2017016). The tissue sections were roasted at 65°C for dewaxing, 3% hydrogen peroxide was added for 10 min to exclude endogenous peroxidase, and the blocking reagent was added after antigen repair. The specimens were incubated with the corresponding primary antibody at 4°C overnight. Then, immunodetection was performed with biotinylated anti-rabbit immunoglobulin for 30 min at room temperature, followed by 3,3'-diaminobenzidine chromogenic as a substrate to visualize the slides and Harris hematoxylin for counterstaining. Positive and negative staining controls were carried out with paraffin tonsil sections using the same antibody above and an appropriate isotype-matched negative control (NC) antibody (rabbit IgG1, ZSGB-BIO, China). The staining was interpreted by two experienced pathologists. IFIH1 staining was mainly in the cytoplasm, PD-L1 staining was mainly in the cytomembrane, and positive signals were of a brown granular appearance.

**Cell culture.** Human breast cancer cell lines MDA-MB-231 and BT-549 (Procell Life Science & Technology, China) were selected as *in vitro* experimental models. The cells were cultured in 10% FBS + DMEM or 10% FBS + RPMI 1640 medium in our laboratory.

**siRNA transfection.** IFIH1 and NC siRNA were designed and purchased by GenePharma (Shanghai, China). The most effective targeted sequences were as follows: siIFIH1 5'-GCACGAGGAAUAAUCUUUATT-3'. Transfection of siRNA was performed by using GP-transfect-Mate transfection reagents (GenePharma, Shanghai) according to the manufacturer's protocol. Cells were collected 48 h after transfection. poly(I:C) (Sigma, Germany) transfection was performed by using Lipofectamine 3000 Transfection Reagent (Invitrogen, Thermo Fisher Scientific) as recommended by the manufacturer's protocol.

**Real-time fluorescent quantitative PCR and western blot.** RNA was isolated from cells using Trizol Reagent (Invitrogen, USA). RNA was then reverse-transcribed to cDNA using a reverse transcription kit (Promega, Go Script™ Reverse Transcription System, #A5001). The cDNA was subsequently PCR amplified using GO Taq qPCR Master Mix (Promega, USA). Taking the DNA obtained by reverse transcription as a template, primers with the best concentration were added, and PCR detection was performed in a 20  $\mu$ l reaction system. The relative mRNA expression was normalized to GAPDH (Forward: 5'-CAAGGCTGAGAAC-

GGGAA-3'; Reverse: 3'-GCATCGCCCCACTTGATTT-5'). The IFIH1 primer (Forward: 5'-TGGGGCATGGAGAATA-CTC-3'; Reverse: 3'-CTGCCCATGTTGCTGTTATG-5') was purchased from Thermo Fisher Scientific (Shanghai, China). The relative expression levels of target genes were determined using the  $2^{-\Delta\Delta Ct}$  method.

The cells were collected after transfection, and total protein was extracted from two kinds of cells using radioimmunoprecipitation assay (RIPA) buffer (Beyotime, China). The protein bands were visualized using an enhanced chemiluminescence (ECL) kit (Beyotime, China). Quantification of protein expression intensities was performed using the ImageJ software. Antibodies involved include anti-IFIH1 (1:1000; Proteintech, 21775-1-AP), anti-GAPDH (1:10000; Proteintech, 10494-1-AP), anti-p-TBK1 (1:1000; CST5483T), anti-p-IRF3 (1:1000; Boster, BM4844), anti-PD-L1 (1:1000; Proteintech, 28076-1-AP), anti-Bcl-2 (1:8000; Proteintech, 12789-1-AP), anti-Bax (1:8000; Proteintech, 50599-2-Ig).

**CCK-8 and plate cloning experiments.** 48 h after transfection, the cell suspension was counted and inoculated on 96-well plates. After 0, 24, 48, 72, and 96 h of adhesion, CCK-8 reagent was added to each well and incubated in an incubator at 37°C for 1h. The absorbance of the reaction mixture at 450 nm was measured using a microplate reader (Tecan, Mannedorf, Switzerland). The experiment was repeated three times. Similarly, after a certain period of time after cell transfection, cell suspensions were prepared and seeded in 6-well plates after counting and cultured for 10–14 days. After clone formation, the cells were treated with 4% paraformaldehyde for fixation. After rinsing with PBS, the cells were stained with crystal violet. Finally, the cell colonies were counted and imaged. The multiplication curve was drawn by GraphPad Prism.

**FITC Annexin V Apoptosis Detection.** All cells were collected, including both the floating cells and the attached cells. Cells were incubated with FITC Annexin V in a buffer containing propidium iodide (PI) (FITC Annexin V Apoptosis Detection Kit I, BD, USA) and detected according to the manufacturer's protocol. Flow cytometry was performed using a Gallios Flow Cytometer (Beckman Coulter, USA), and the data were analyzed using FLOWJO software (BD, USA).

**Statistical analysis.** The measurement data were expressed as mean  $\pm$  standard deviation, and the Chi-square test was used to compare the two groups of data. Spearman correlation analysis was used to investigate the correlation between IFIH1 and PD-L1 expression levels. A p-value  $<0.05$  was considered statistically significant.

## Results

**Higher levels of serum interferons and tissue IFIH1 indicate better clinical outcomes in TNBC patients.** Serum samples from eight patients with TNBC were analyzed for pro-inflammatory cytokines and immune cell subsets.

Samples were collected before treatment with neoadjuvant docetaxel and carboplatin combined with apatinib. Compared with non-pCR cases (5/8), patients who achieved pCR (3/8) had significantly higher expression levels of IFN- $\gamma$ , IFN- $\alpha$ , TNF- $\alpha$ , and IL-6 ( $p<0.0001$ ,  $p=0.027$ ,  $p=0.0309$ , and  $p=0.0074$ , separately). There was no significant difference in immune cell subsets between the pCR and the non-pCR group (Figure 1A). The protein-protein interaction network involving IFN- $\alpha$  and IFN- $\beta$ , two major members of the type I interferon family, was subsequently subjected to analysis. The findings revealed a significant interaction between IFIH1 and type I interferon as well as its associated receptors (Figures 1B, 1C).

Using the TIMER2.0 database, we compared the mRNA levels of IFIH1 in pan-cancer tissues based on RNA sequencing data from TCGA and Genotype-Tissue Expression (GTEx) database. The results showed that IFIH1 expression was significantly upregulated in many types of cancer tissue, including BC. The expression of IFIH1 between BC tissues and normal tissues according to TCGA data was compared using the UALCAN online tool. Analysis of data from 1,097 cases of invasive BC and 114 normal breast tissue samples revealed that the expression level of IFIH1 was increased in cancer tissues compared to normal tissues. We found that IFIH1 expression was higher in all BC tissues compared with normal tissues, with TNBC showing the most significant increase. In addition, we assessed the expression of IFIH1 protein using the HPA database and observed that IFIH1 was expressed at a low level in normal breast tissues but moderately or highly expressed in BC tissues (Supplementary Figure S1).

To further verify the expression patterns of IFIH1, immunohistochemical staining was conducted on 39 BC tissues from the clinical specimen bank. The baseline data of the 39 patients were relatively balanced. As shown in Figure 2, IFIH1 exhibited a heterogeneous subcellular distribution in both tumor cytoplasm and cell membranes of BC tumors. Patients were classified into groups based on their IFIH1 expression score, with 46.2% (18/39) showing relatively high and 53.8% (21/39) showing low expression. However, contrary to the results of the database analysis, we did not find any correlation between IFIH1 expression and patient age, tumor size, or lymph node status. This discrepancy may be attributed to the limited number of patients included in this study (Table 1).

The Kaplan-Meier Plotter mapping database was used to evaluate the relationship between IFIH1 expression and the prognosis of patients with TNBC. TNBC patients were grouped according to the best truncation value, and RFS and OS were compared between the groups. The survival curve (Supplementary Figure S2) showed that TNBC patients with high IFIH1 expression had better OS compared with patients with low IFIH1 expression, and the difference was statistically significant. Relapse-free survival was also significantly different. This suggests that high expression levels of IFIH1

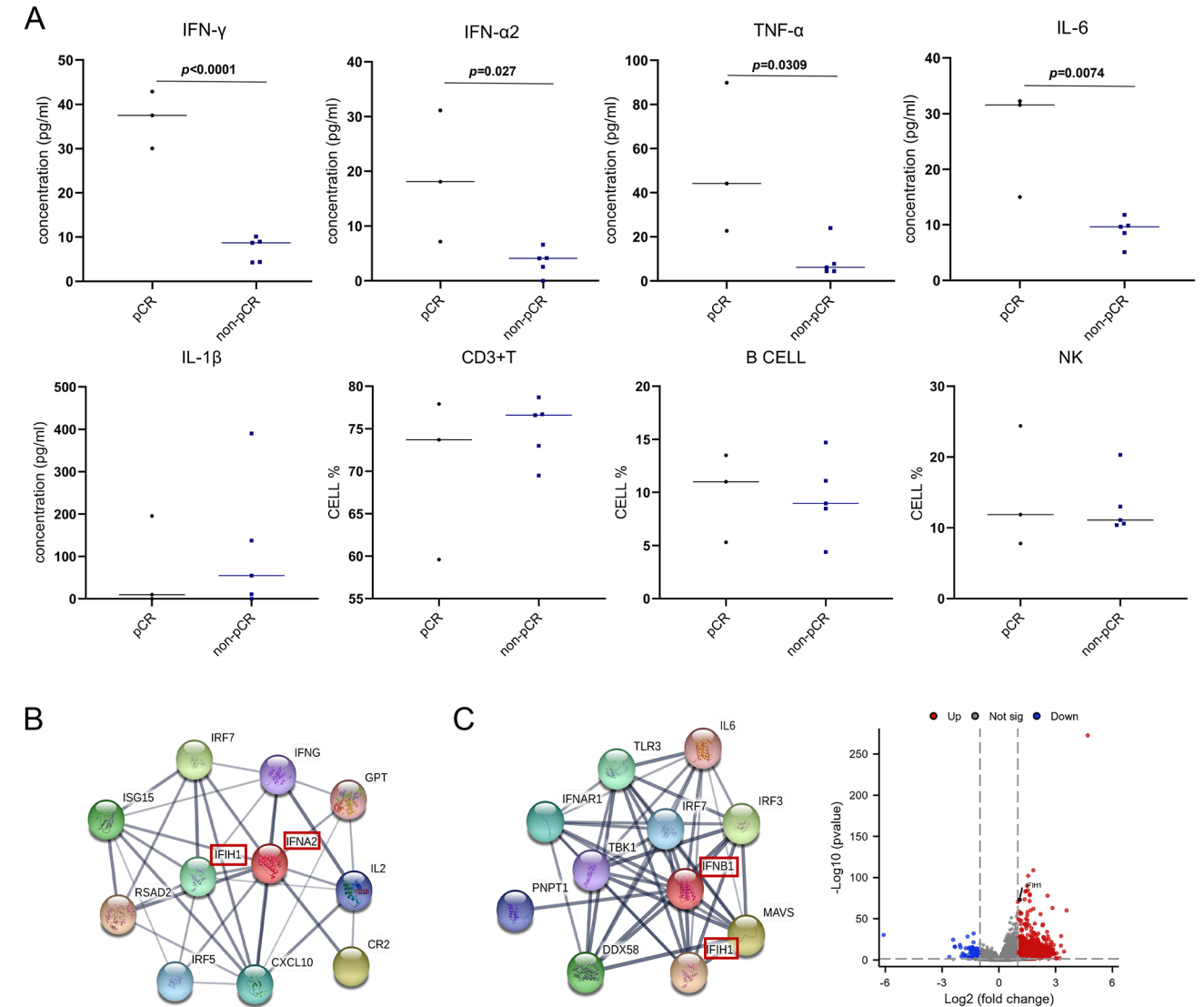


Figure 1. Changes of serum cytokines level and immune cell subsets in patients with TNBC and IFIH1 expression in BC. A) TNBC patients with pCR had higher serum interferons and other cytokines expression levels. B, C) PPI mapping suggested a significant interaction between IFIH1, type I interferon, and its related receptors.

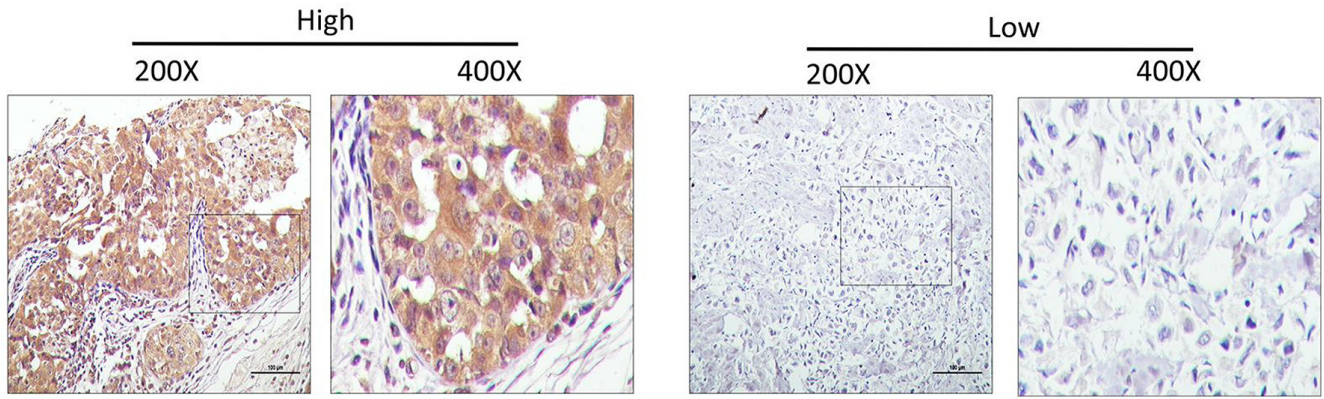


Figure 2. Representative IHC staining patterns of IFIH1 in BC tissues. Positive, (magnification  $\times 200$ ,  $\times 400$ ); negative, (magnification  $\times 200$ ,  $\times 400$ ).



may greatly enhance the ability of patients with TNBC to benefit clinically from treatment, thereby improving their prognosis.

**IFIH1 promotes apoptosis and PD-L1 in BC.** To better understand the potential anti-tumor mechanism of IFIH1 in BC, we conducted further analysis on the genes co-expressed with IFIH1 and related pathways using TCGA data. We divided the samples into two groups based on the median expression level of IFIH1: a high expression group (samples with expression levels higher than the median) and a low expression group (samples with expression levels lower than the median). We then identified the differentially expressed genes between these two groups. The criteria used to determine differential gene expression was  $\log_2$  (Fold Change)  $> 1.5$ . A volcano map was constructed to visualize the differentially expressed genes, of which 193 genes were upregulated and 62 genes were downregulated (Figure 3A). In

addition, we used the STRING online database to construct a protein-protein interaction network for the top differentially expressed genes related to IFIH1. This network included key genes such as TANK-binding kinase 1 (TBK1), mitochondrial antiviral signaling protein (MAVS), and interferon regulatory factor 3 (IRF3) (Figure 3B). Through gene ontology functional annotation analysis of the differential genes, we found that IFIH1 and its co-expressed genes were enriched in the extracellular region of cells, autophagosome, peroxisome, and other structures, and jointly participated in the innate and adaptive immune processes of the body and the production of interferons, as well as cytokine regulation and related biological processes (Supplementary Figure S3). Furthermore, we employed gene set enrichment analysis to pinpoint pivotal IFIH1-associated pathways involved in BC. A plethora of involved in type I interferon pathway, apoptosis signaling, and PD-1 signaling were identified (Figure 3C).

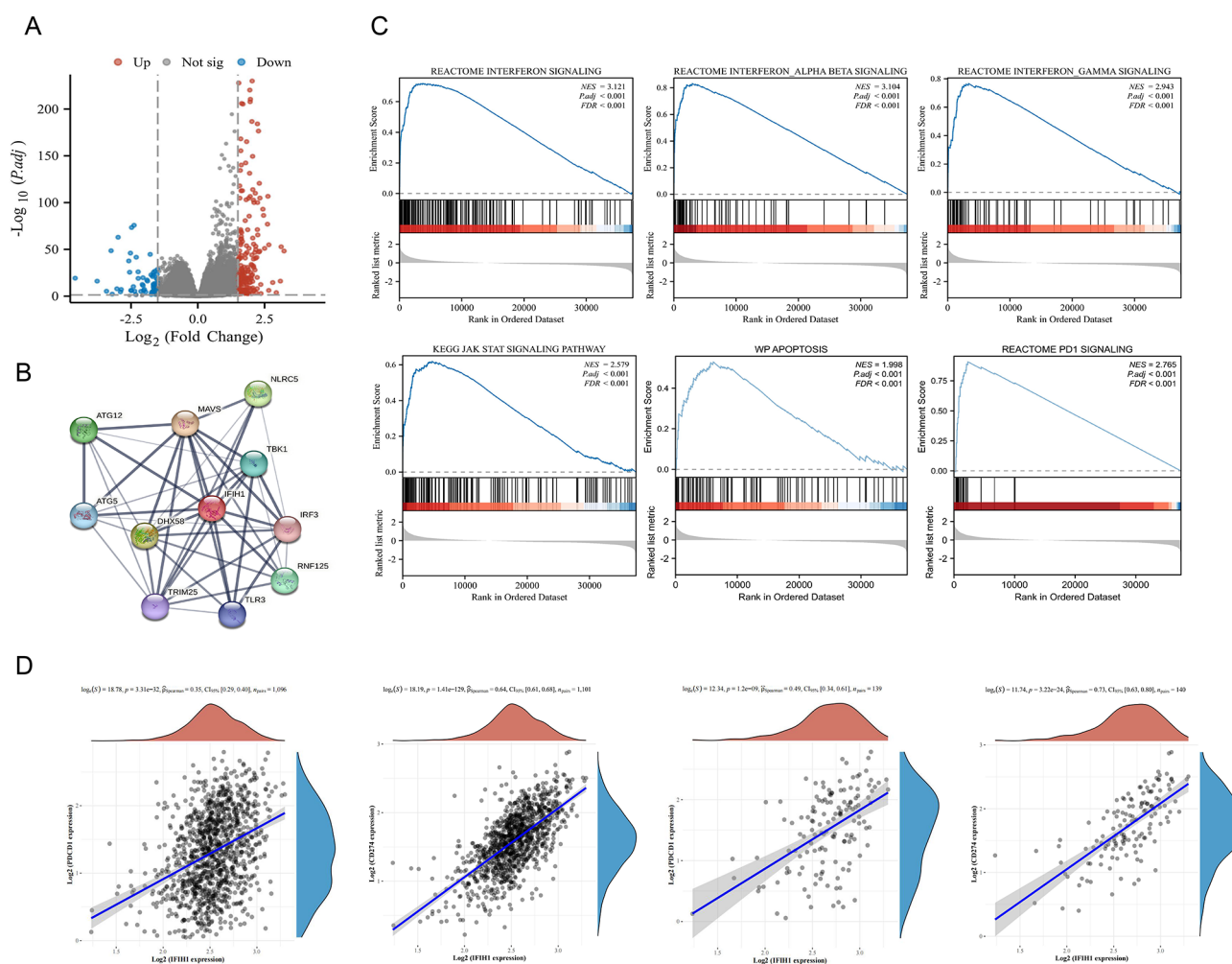


**Figure 3.** IFIH1 coexpression genes and pathways enrichment in BC. A) Volcano plot of IFIH1-associated DEGs in TCGA BC database. B) The PPI network of the top IFIH1 DEGs; C) GSEA functional enrichment of IFIH1 associated DEGs in BC. D) Relationship between IFIH1 expression level and immune checkpoint inhibitors in BC/TNBC.

**Table 1. IFIH1 expression according to the clinicopathological characteristics of BC patients (n=39).**

Characteristics	Low expression of IFIH1	High expression of IFIH1	p-value
n	21	18	
Age, n (%)			1.000
≥50	14 (53.8%)	12 (46.2%)	
<50	7 (53.8%)	6 (46.2%)	
Tumor size, n (%)			0.528
≤2.0	8 (47.1%)	9 (52.9%)	
>2.0	13 (59.1%)	9 (40.9%)	
TNM pathological stage, n (%)			0.307
I-II	12 (46.2%)	14 (53.8%)	
III	9 (69.2%)	4 (30.8%)	
Lymph nodes involved, n (%)			0.742
≤3	12 (50%)	12 (50%)	
>3	9 (60%)	6 (40%)	
Intravascular tumor thrombus, n (%)			1.000
Negative	15 (53.6%)	13 (46.4%)	
Positive	6 (54.5%)	5 (45.5%)	
ER, n (%)			0.323
Negative	10 (66.7%)	5 (33.3%)	
Positive	11 (45.8%)	13 (54.2%)	
PR, n (%)			0.113
Negative	14 (66.7%)	7 (33.3%)	
Positive	7 (38.9%)	11 (61.1%)	
HER-2, n (%)			1.000
Negative	13 (52%)	12 (48%)	
Positive	8 (57.1%)	6 (42.9%)	
Ki-67, n (%)			0.334
High (>30%)	11 (64.7%)	6 (35.3%)	
Low (≤30%)	10 (45.5%)	12 (54.5%)	
Molecular subtype, n (%)			0.187
Luminal	12 (70.6%)	5 (29.4%)	
HER2	6 (42.9%)	8 (57.1%)	
TNBC	3 (37.5%)	5 (62.5%)	

**Table 2. Correlation between IFIH1 and PD-L1 expression in BC tissues.**

Characteristics	Low expression of IFIH1	High expression of IFIH1	r	p-value
n	21	18		
PD-L1 expression, n (%)			0.658	<0.0001
Low	20 (71.4%)	8 (28.6%)		
High	1 (9.1%)	10 (90.9%)		

Cancer immunotherapy, specifically immune checkpoint inhibitors, holds great promise as a treatment option for BC. Previous studies on various tumor types have demonstrated that IFIH1 can activate type I and type II interferon signals, thereby enhancing the anti-tumor immune response, inhibiting cell proliferation, and inducing cell apoptosis to effectively inhibit tumor growth. To further investigate the role of IFIH1 expression in immunotherapy, we also evaluated the relationships between mRNA levels of immune

checkpoint genes (PD-1, PD-L1) and IFIH1 expression in both BC overall and TNBC. Our analysis showed that there was a significant correlation between IFIH1 expression and immune checkpoint expression in TCGA dataset, with PD-L1 showing the strongest correlation (Figure 3D). Therefore, IFIH1 may regulate PD-L1 expression through a certain pathway in BC.

**IFIH1 regulates apoptosis and PD-L1 expression through the TBK1/IRF3 signaling pathway.** To investigate the impact of IFIH1 expression on BC cell function and downstream pathways, we performed gene knockdown experiments in the MDA-MB-231 and BT-549 cell lines using RNA interference technology. The efficiency of knockdown was confirmed. Our findings revealed a significant downregulation of IFIH1 RNA expression and protein expression in knockdown (si-IFIH1) cells compared with the control (si-NC) group (Figures 4A, 4B). As shown in Figure 3C, there was a correlation between IFIH1 expression and the apoptosis pathway; to further explore this association, we conducted CCK-8 cell proliferation and plate cloning experiments. As anticipated, the results demonstrated that the knockdown of IFIH1 significantly enhanced cell proliferation and the ability to form colonies (Figures 4C, 4D).

We further analyzed the impact of IFIH1 on the activity of the apoptosis pathway and immune-related pathways at the protein level. First, western blotting was used to analyze changes in the expression of apoptosis-related proteins and PD-L1 following IFIH1 knockdown. The results revealed that the knockdown of IFIH1 led to decreased expression of the classical pro-apoptotic protein Bax, whereas there was an increase in expression of anti-apoptotic protein Bcl-2. In addition, decreased expression of IFIH1 caused a decrease in expression of PD-L1 (Figure 4E). The correlation between IFIH1 and PD-L1 was then analyzed by immunohistochemistry. This showed that the relatively high and low expression levels of PD-L1 in BC tissues were 28.2% (11/39) and 71.8% (28/39), respectively, and there was a significant positive correlation with the expression of IFIH1 (Figure 5, Table 2). This was consistent with the results of the previous database analysis.

To elucidate the mechanism by which IFIH1 affects apoptosis and PD-L1 expression in BC cells, we evaluated the phosphorylation status of key proteins involved in innate-immune-related signaling pathways. Levels of phosphorylated TBK1 and phosphorylated IRF3 were markedly reduced in IFIH1-knockdown cells ( $p < 0.05$ ), but total TBK1 (pan-TBK1) and total IRF3 (pan-IRF3) levels remained unchanged (Figure 6A). Poly(I:C) is recognized as an agonist of IFIH1. We further validated the alterations in the regulatory pathways by transfecting poly(I:C) into the MDA-MB-231 cell line. After transfection, the expression of IFIH1 increased in a dose-dependent manner. Subsequently, there was a gradual increase in the expression of the classical pro-apoptotic protein Bax with increasing transfection concentration, while the expression of the anti-apoptotic

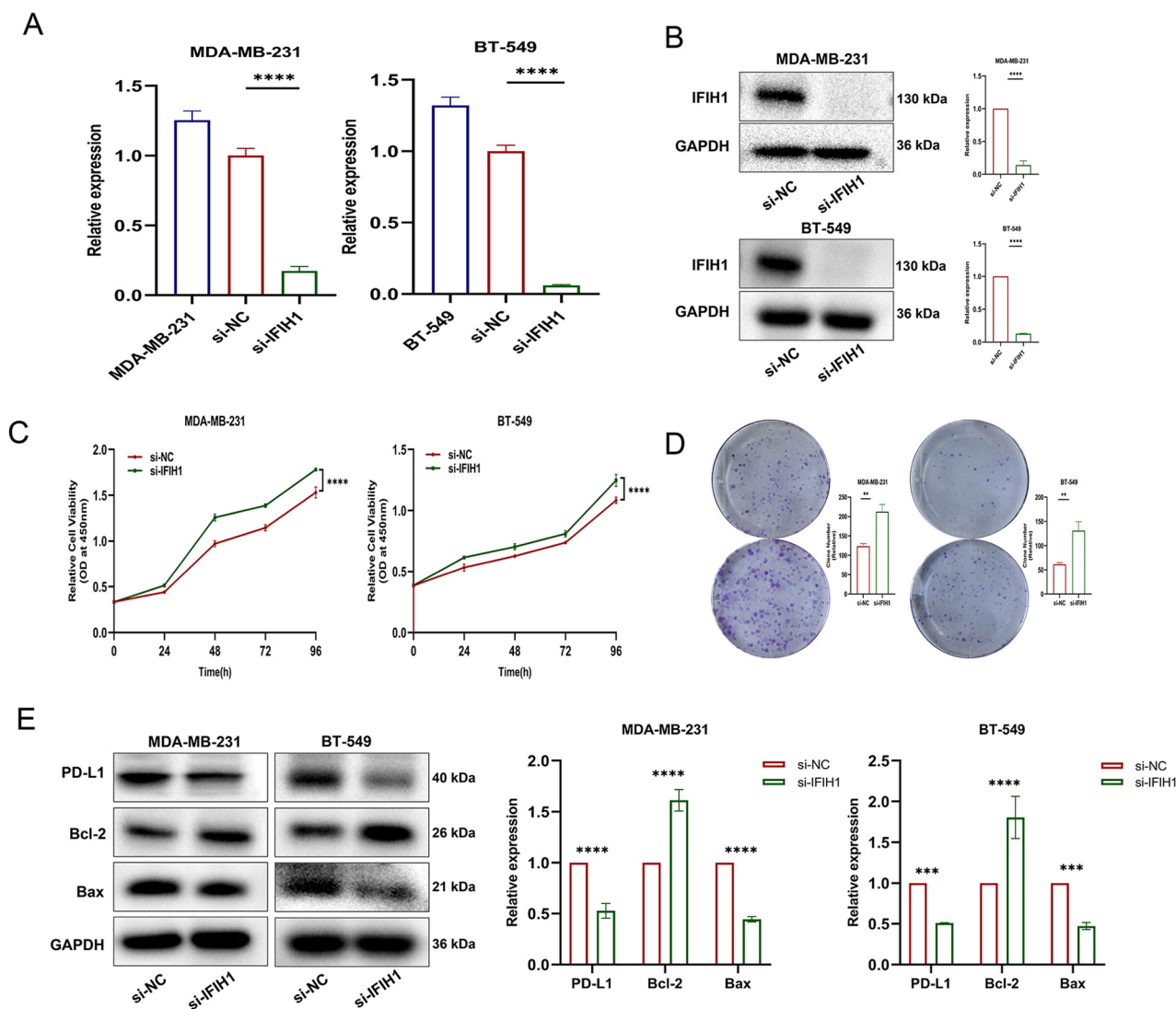


Figure 4. IFIH1 regulated cancer cell apoptosis and PD-L1 expression. A, B) Efficiency of si-IFIH1 knockdown in the MDA-MB-231 and BT-549 cell lines. C, D) The effect of IFIH1 knockdown on the proliferation of MDA-MB-231/BT-549 cells was verified by CCK-8 and plate cloning experiments. E) Western Blot verified the changes of downstream apoptotic pathway proteins and PD-L1 after transfection with si-IFIH1.

protein Bcl-2 decreased gradually (Figure 6B). The apoptosis rate was significantly elevated upon IFIH1 activation, as demonstrated by flow cytometry following poly(I:C) transfection (Figure 6C). Additionally, upregulated expression of PD-L1 was observed following transfection with poly(I:C) (Figure 6B).

The expression of IFIH1 was upregulated following poly(I:C) transfection, leading to the activation of TBK1 and IRF3 phosphorylation (Figure 6D). We used the JASPAR database to predict and analyze transcription factor-binding sites on the PD-L1 promoter. Our analysis revealed the presence of two potential IRF3-binding sites in the PD-L1 promoter (Figure 6E). Overall, these results indicate that inhibition of IFIH1 expression can inhibit PD-L1 expression

and apoptosis by inhibiting the transcriptional process initiated by the TBK1/IRF3 signaling pathway.

## Discussion

In this study, we found that IFIH1 is an important regulator involved in cancer apoptosis. IFIH1 and its related pathways may provide new targets and prognostic markers for patients with TNBC. We analyzed the potential pathways of genes co-expressed with IFIH1 in BC and found that they primarily comprised interferon signaling, apoptosis signaling, and immunosuppressive point-related pathways in BC. Bcl-2 is an anti-apoptotic protein located on the mitochondrial membrane, and Bax is a pro-apoptotic protein



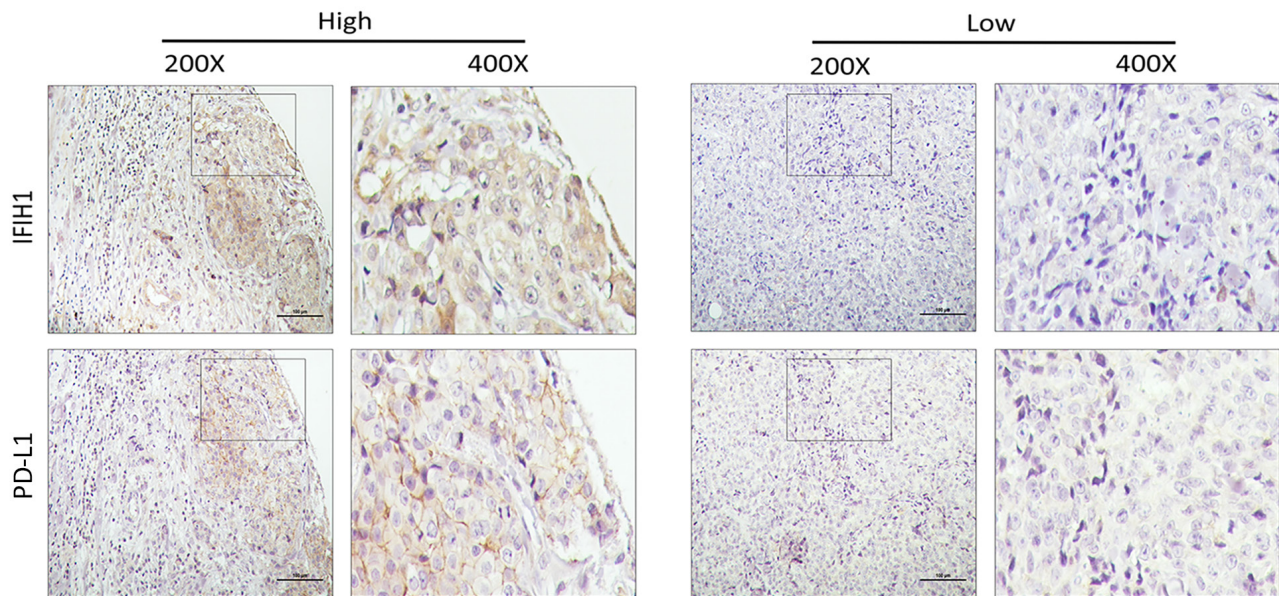


**Figure 5.** Representative IFIH1 and PD-L1 expression in BC tissues by IHC staining. Positive, (magnification  $\times 200$ ,  $\times 400$ ); negative, (magnification  $\times 200$ ,  $\times 400$ ).

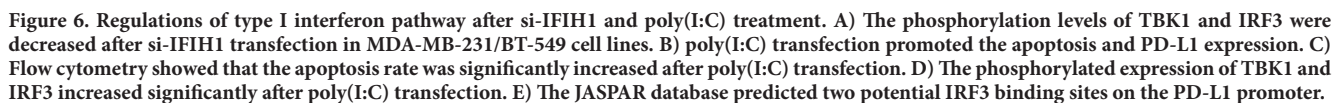
that plays a key part in the inherent apoptosis pathway [15]. Previous studies have shown that IFIH1 can activate the caspase 3/7 pathway to induce apoptosis of liver cancer cells and inhibit the growth of transplanted liver cancer tumors in mice [16]. Activation of IFIH1/MAVS and thrombolytic protein NOX cooperates with the regulation of melanoma cell death and inhibits lung metastasis of melanoma in mice. It has also been found that tumor cells are highly sensitive to RIG-I/IFIH1-induced apoptosis, whereas non-malignant cells are protected by upregulation of endogenous Bcl-xL [17]. Retinoic acid-inducible gene I (RIG-I)/IFIH1 activation-mediated apoptosis induction is independent of p53 mutations in cancer cells and has an important role in apoptotic resistance to chemotherapy or radiotherapy. In addition, in melanoma cells, RIG-I and IFIH1 activate a p53-independent Noxa pro-apoptotic signaling pathway that is independent of the type I interferon response [18]. Here, western blotting was used to analyze the changes in the expression of apoptosis-related proteins after IFIH1 knockdown; the expression of classical pro-apoptotic protein Bax decreased, whereas that of anti-apoptotic protein Bcl-2 increased after IFIH1 knockdown, further supporting the role of IFIH1 in the development and progression of BC.

In mammalian cells, key cytoplasmic nucleic acid sensing pathways include cGAS-STING and RLRs-MAVS, which are responsible for detecting cytoplasmic DNA and RNA. RIG-I-like receptors (RLRs) form a family of RNA receptors including RIG-I, IFIH1, and laboratory of genetics and physiology 2 (LGP2). The IFIH1 protein, located in the cytoplasm, is a dsRNA-dependent ATP enzyme, that recog-

nizes long-stranded high-order dsRNA structures [19]. This recognition triggers the formation of complexes with MAVS, inducing interferons through phosphorylation of IRF3 and notifying neighboring cells of viral infection. The RLR signaling pathway, a key component of the innate immune system, has been implicated in a previously unrecognized role connecting bacterial infections, innate immunity, and the metastatic progression of cancer. This groundbreaking finding elucidates potential new avenues for therapeutic intervention in breast cancer management [20]. RLR agonists are anticipated to have applications in cancer therapy, as they can induce tumor cell death and enhance tumor immunogenicity by upregulating interferons or pro-inflammatory cytokines [21, 22]. Therefore, IFIH1 activation represents a potential source of predictive biomarkers and therapeutic targets in cancer.

BC exhibits more immunocold tumor characteristics and lacks effective immunotherapy measures [23]. Therefore, investigating the immune activation and escape mechanisms of BC and identifying predictive biomarkers and therapeutic targets are crucial for more accurate BC patient treatment. In the innate immune response, the IFIH1 signaling pathway interacts with the adapter MAVS, recruiting TBK1. The phosphorylation cascade leads to signal transduction, resulting in IRF3 and IRF7 production, usually inducing interferon production and subsequently activating interferon-stimulated genes (ISGs) target genes [24]. Transcriptional regulators, including IRF3, have been shown to regulate PD-L1 expression. In melanoma, IRF3 promotes ultraviolet (UV) induction of PD-L1 by forming a transcrip-





Our study had some limitations. More clinical specimens need to be collected to provide more evidence to verify the

association of IFIH1 with clinical factors in BC, especially TNBC; in particular, to verify the association of IFIH1 with immune invasion and response to immune checkpoint blockade. In addition, more studies need to be performed to further elucidate the regulation of IFIH1 in TNBC.

In summary, IFIH1 is an important RNA sensor, and its related signaling pathways could have key roles in improving treatment outcomes and prognosis in TNBC. The results presented here provide valuable information for clinical diagnosis and tumor immunotherapy and indicate a new direction for potential target drug development.

**Supplementary information** is available in the online version of the paper.

**Acknowledgments:** This work was supported by the Natural Science Foundation of Hebei Province, No. H2023206441 and No. H2022206378. The authors thank Ms. Jianxin Wang, Ms. Chunxiao Li, and the investigators for excellent data handling, and all the patients for participating in this study.

## References

- [1] WU S, LU J, ZHU H, WU F, MO Y et al. A novel axis of circKIF4A-miR-637-STAT3 promotes brain metastasis in triple-negative breast cancer. *Cancer Lett* 2024; 581: 216508. <https://doi.org/10.1016/j.canlet.2023.216508>
- [2] HUANG X, SONG C, ZHANG J, ZHU L, TANG H. Circular RNAs in breast cancer diagnosis, treatment and prognosis. *Oncol Res* 2023; 32: 241–249. <https://doi.org/10.32604/or.2023.046582>
- [3] DE CICCIO P, ERCOLANO G, IANARO A. The New Era of Cancer Immunotherapy: Targeting Myeloid-Derived Suppressor Cells to Overcome Immune Evasion. *Front Immunol* 2020; 11: 1680. <https://doi.org/10.3389/fimmu.2020.01680>
- [4] LUO J, SOLIMINI NL, ELLEDGE SJ. Principles of cancer therapy: oncogene and non-oncogene addiction. *Cell* 2009; 136: 823–837. <https://doi.org/10.1016/j.cell.2009.02.024>
- [5] ROULOIS D, LOO YAU H, SINGHANIA R, WANG Y, DANESH A et al. DNA-Demethylating Agents Target Colorectal Cancer Cells by Inducing Viral Mimicry by Endogenous Transcripts. *Cell* 2015; 162: 961–973. <https://doi.org/10.1016/j.cell.2015.07.056>
- [6] CHIAPPINELLI KB, STRISSEL PL, DESRICHARD A, SLAMON DJ, WOLCHOK JD et al. Inhibiting DNA Methylation Causes an Interferon Response in Cancer via dsRNA Including Endogenous Retroviruses. *Cell* 2015; 162: 974–986. <https://doi.org/10.1016/j.cell.2015.07.011>
- [7] BESCH R, POECK H, HOHENAUER T, SENFT D, HÄCKER G et al. Proapoptotic signaling induced by RIG-I and MDA-5 results in type I interferon-independent apoptosis in human melanoma cells. *J Clin Invest* 2009; 119: 2399–2411. <https://doi.org/10.1172/JCI37155>
- [8] SMYTH DJ, COOPER JD, BAILEY R, FIELD S, BURREN O et al. A genome-wide association study of nonsynonymous SNPs identifies a type 1 diabetes locus in the interferon-induced helicase (IFIH1) region. *Nat Genet* 2006; 38: 617–619. <https://doi.org/10.1038/ng1800>
- [9] SETH RB, SUN L, EA CK, CHEN ZJ. Identification and characterization of MAVS, a mitochondrial antiviral signaling protein that activates NF-kappaB and IRF3. *Cell* 2005; 122: 669–682. <https://doi.org/10.1016/j.cell.2005.08.012>
- [10] WANG L, ZHANG X, MA X, REN X, MA X et al. Elevated Sera IL-6 and NK-T Cells Associated With Increased Pathological Complete Response in HER2-positive Breast Cancer With Carboplatin-based Neoadjuvant Therapy. *Altern Ther Health Med* 2023; 29: 246–253.
- [11] LI T, FU J, ZENG Z, COHEN D, LI J et al. TIMER2.0 for analysis of tumor-infiltrating immune cells. *Nucleic Acids Res* 2020; 48: W509–W514. <https://doi.org/10.1093/nar/gkaa407>
- [12] CHANDRASHEKAR DS, BASHEL B, BALASUBRAMANYA SAH, CREIGHTON CJ, PONCE-RODRIGUEZ I et al. UALCAN: A Portal for Facilitating Tumor Subgroup Gene Expression and Survival Analyses. *Neoplasia* 2017; 19: 649–658. <https://doi.org/10.1016/j.neo.2017.05.002>
- [13] UHLÉN M, FAGERBERG L, HALLSTRÖM BM, LINDSKOG C, OKSVOLD P et al. Proteomics. Tissue-based map of the human proteome. *Science* 2015; 347: 1260419. <https://doi.org/10.1126/science.1260419>
- [14] GYÖRFFY B, LANCZKY A, EKLUND AC, DENKERT C, BUDCZIES J et al. An online survival analysis tool to rapidly assess the effect of 22,277 genes on breast cancer prognosis using microarray data of 1,809 patients. *Breast Cancer Res Treat* 2010; 123: 725–731. <https://doi.org/10.1007/s10549-009-0674-9>
- [15] TANG Y, TIAN W, ZHENG S, ZOU Y, XIE J et al. Dissection of FOXO1-Induced LYPLAL1-DT Impeding Triple-Negative Breast Cancer Progression via Mediating hnRNP/β-Catenin Complex. *Research* 2023; 6: 0289. <https://doi.org/10.34133/research.0289>
- [16] PENG S, GENG J, SUN R, TIAN Z, WEI H. Polyinosinic-polycytidylic acid liposome induces human hepatoma cells apoptosis which correlates to the up-regulation of RIG-I like receptors. *Cancer Sci* 2009; 100: 529–536. <https://doi.org/10.1111/j.1349-7006.2008.01062.x>
- [17] BESCH R, POECK H, HOHENAUER T, SENFT D, HÄCKER G et al. Proapoptotic signaling induced by RIG-I and MDA-5 results in type I interferon-independent apoptosis in human melanoma cells. *J Clin Invest* 2009; 119: 2399–2411. <https://doi.org/10.1172/JCI37155>
- [18] POECK H, BESCH R, MAIHOFER C, RENN M, TORMO D et al. 5'-Triphosphate-siRNA: turning gene silencing and Rig-I activation against melanoma. *Nat Med* 2008; 14: 1256–1263. <https://doi.org/10.1038/nm.1887>
- [19] KOVACSOVICS M, MARTINON F, MICHEAU O, BODMER JL, HOFMANN K et al. Overexpression of Helicard, a CARD-containing helicase cleaved during apoptosis, accelerates DNA degradation. *Curr Biol* 2002; 12: 838–843. [https://doi.org/10.1016/s0960-9822\(02\)00842-4](https://doi.org/10.1016/s0960-9822(02)00842-4)
- [20] ZHAO H, ZHANG L, DU D, MAI L, LIU Y et al. The RIG-I-like receptor signaling pathway triggered by *Staphylococcus aureus* promotes breast cancer metastasis. *Int Immunopharmacol* 2024; 142: 113195. <https://doi.org/10.1016/j.intimp.2024.113195>

- [21] WU J, CHEN ZJ. Innate immune sensing and signaling of cytosolic nucleic acids. *Annu Rev Immunol* 2014; 32: 461–488. <https://doi.org/10.1146/annurev-immunol-032713-120156>
- [22] CHEN Q, SUN L, CHEN ZJ. Regulation and function of the cGAS-STING pathway of cytosolic DNA sensing. *Nat Immunol* 2016; 17: 1142–1149. <https://doi.org/10.1038/ni.3558>
- [23] OU X, TAN Y, XIE J, YUAN J, DENG X et al. Methylation of GPRC5A promotes liver metastasis and docetaxel resistance through activating mTOR signaling pathway in triple negative breast cancer. *Drug Resist Updat* 2024; 73: 101063. <https://doi.org/10.1016/j.drug.2024.101063>
- [24] BIANCOLELLA M, TESTA B, BAGHERNAJAD SALEHI L, D'APICE MR, NOVELLI G. Genetics and Genomics of Breast Cancer: update and translational perspectives. *Semin Cancer Biol* 2021; 72: 27–35. <https://doi.org/10.1016/j.semincancer.2020.03.013>
- [25] CAO J, YAN Q. Cancer Epigenetics, Tumor Immunity, and Immunotherapy. *Trends Cancer* 2020; 6: 580–592. <https://doi.org/10.1016/j.trecan.2020.02.003>
- [26] AU-YEUNG N, MANDHANA R, HORVATH CM. Transcriptional regulation by STAT1 and STAT2 in the interferon JAK-STAT pathway. *JAKSTAT* 2013; 2: e23931. <https://doi.org/10.4161/jkst.23931>
- [27] DUEWELL P, BELLER E, KIRCHLEITNER SV, TINA A, HELENE B et al. Targeted activation of melanoma differentiation-associated protein 5 (IFIH1) for immunotherapy of pancreatic carcinoma. *Oncoimmunology* 2015; 4: e1029698. <https://doi.org/10.1080/2162402X.2015.1029698>

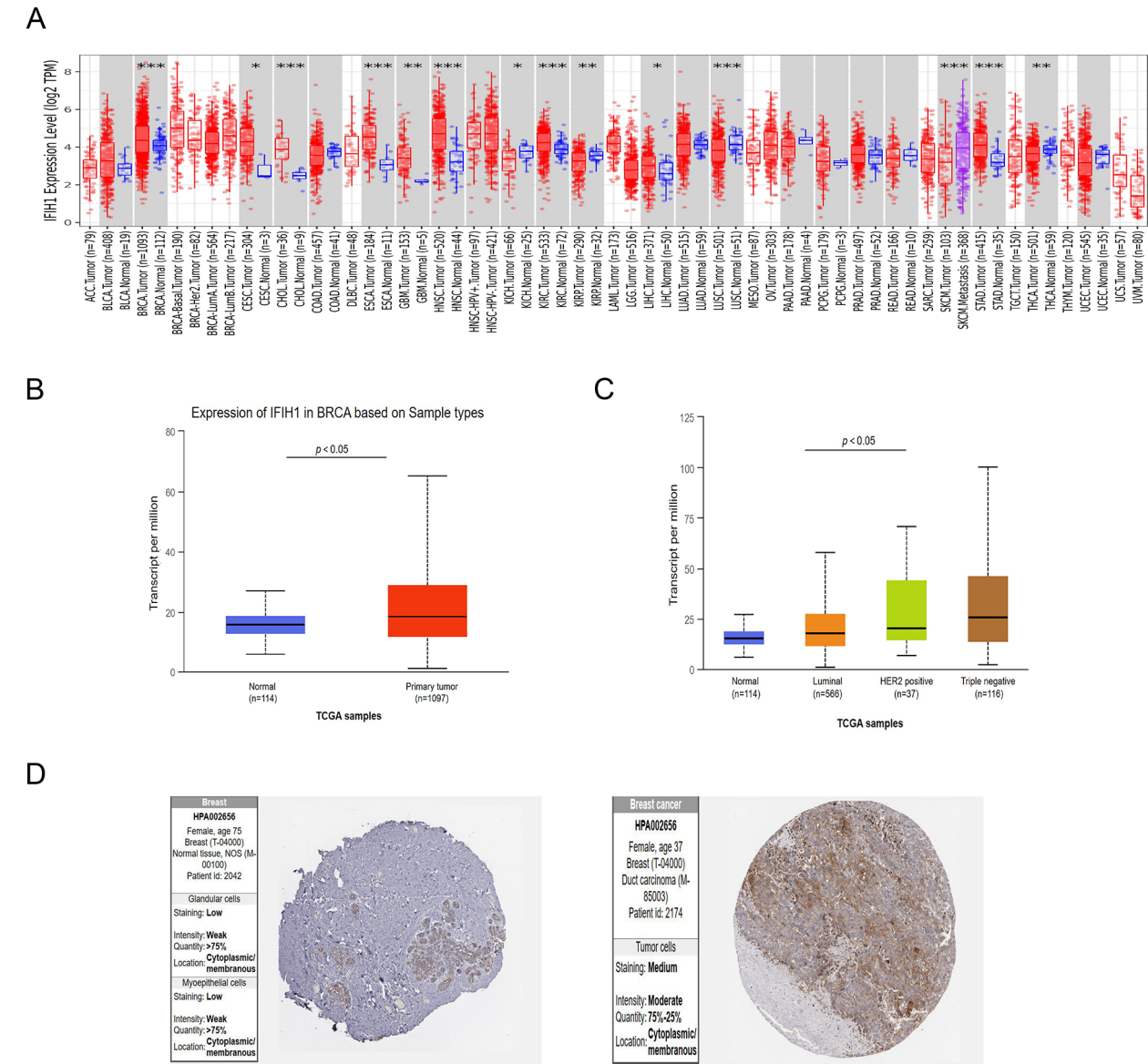


[https://doi.org/10.4149/neo\\_2024\\_240614N255](https://doi.org/10.4149/neo_2024_240614N255)

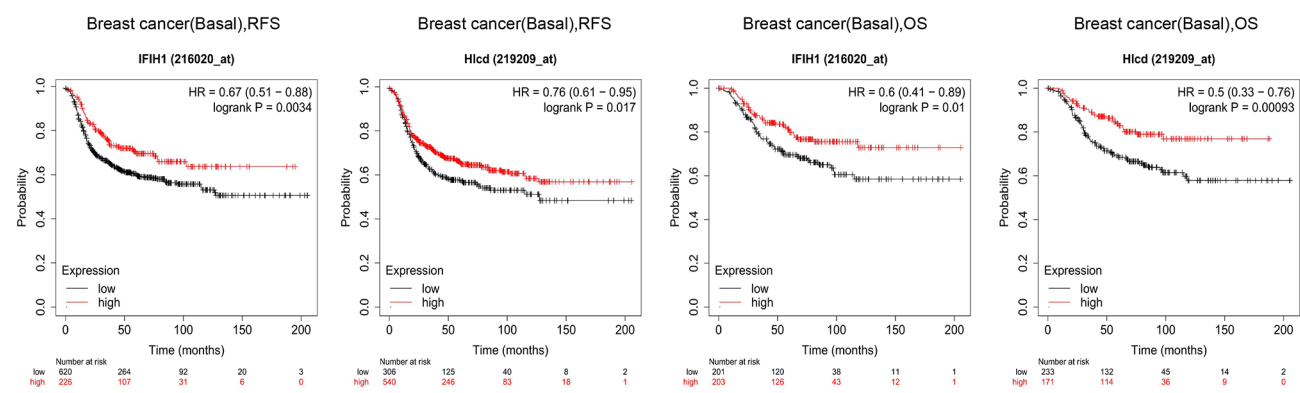
# IFIH1 promotes apoptosis through the TBK1/IRF3 pathway in triple-negative breast cancer

Chao SHI<sup>1</sup>, Xiaohan WANG<sup>1</sup>, Jingping LI<sup>2</sup>, Shang WU<sup>1</sup>, Zhihui LIU<sup>3</sup>, Xiaofei REN<sup>1</sup>, Xiangmei ZHANG<sup>2,4,\*</sup>, Yunjiang LIU<sup>1,2,\*</sup>

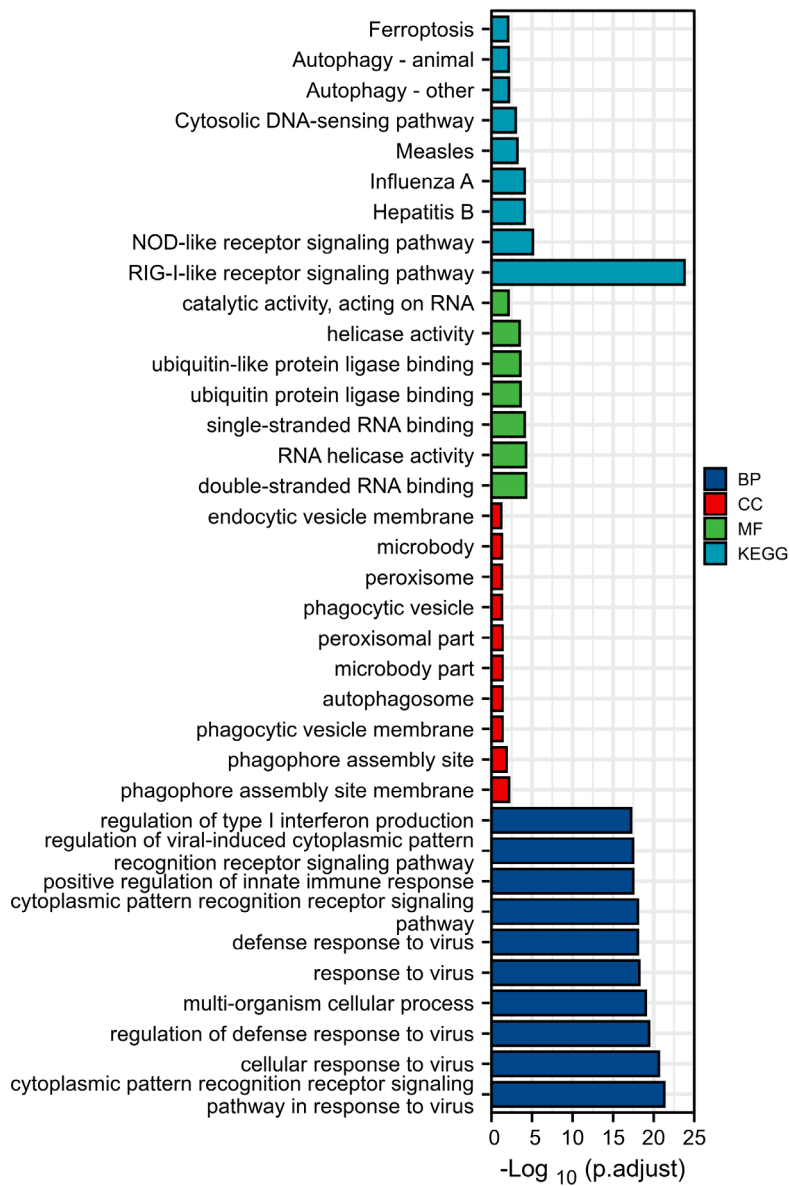
## Supplementary Information



Supplementary Figure S1. A) The expression of IFIH1 in different tumors from the Tumor Immune Estimation Resource (TIMER 2.0), B) IFIH1 expression in BC and normal tissue from UALCAN, C) Correlation between IFIH1 expression level and different subtypes, D) IFIH1 protein levels in normal and breast cancer tissues based on immunohistochemistry data from the HPA database.



Supplementary Figure S2. RFS and OS survival curves of triple-negative breast cancer in the Kaplan-Meier plotter database.



Supplementary Figure S3. Gene ontology functional annotation analysis of the differential genes.